

Article

Enhancement of Characteristics of Field Asymmetric Ion Mobility Spectrometer with Laser Ionization for Detection of Explosives in Vapor Phase

Vitalii A. Kostarev *, Gennadii E. Kotkovskii, Alexander A. Chistyakov and Artem E. AkmalovMoscow Engineering Physics Institute, National Research Nuclear University, 31, Kashirskoe Sh.,
Moscow 115409, Russia; geko@mail.ru (G.E.K.); chistaa@mail.ru (A.A.C.); akmalovtm@gmail.com (A.E.A.)

* Correspondence: vakostarev@mail.ru; Tel.: +7-926-255-3778

Received: 22 August 2020; Accepted: 25 September 2020; Published: 27 September 2020



Abstract: Ion mobility spectrometry instrumentation today is widespread in the area of transport security and counterterrorism. This method of detection of explosive substances is highly appreciated for the existence of portable detectors capable of detecting concentrations of 10^{-13} – 10^{-14} g/cm³ at atmospheric pressure using traditional ionization methods including corona discharge and beta radiation. However, low vapor pressure of some explosives imposes requirements on limit of detection (LOD) down to 10^{-15} – 10^{-16} g/cm³. In this paper we compare a radioactive ⁶³Ni ionization source with a laser ionization source and reveal the parameters of laser ionization of a group of explosives, namely trinitrotoluene (TNT), cyclotrimethylene-trinitramine (RDX), cyclotetramethylene-tetranitramine (HMX) and pentaerythritol tetranitrate (PETN), which can reduce the limit of detection of portable devices. A laser ionization source can provide a higher signal to noise ratio than radioactive ⁶³Ni at optimal intensity of laser radiation for PETN and HMX of 3×10^7 W/cm² and 2.5×10^7 W/cm², respectively. Limits of detection were estimated: 3×10^{-15} g/cm³ for RDX, 8×10^{-15} g/cm³ for PETN and less than 3×10^{-15} g/cm³ for HMX. These results are promising to further improve the capabilities of detectors of low volatility explosives without sacrificing portability, light weight and reasonable cost of the laser source.

Keywords: FAIMS; ion source; ⁶³Ni; laser ionization; limit of detection; TNT; RDX; HMX; PETN

1. Introduction

State-of-the-art detectors of explosives are developed nowadays involving a wide range of physical and chemical methods including gas-analytical, nuclear-physical, electromagnetic and biological. One of the most challenging problems is detection of explosives in the vapor phase. In [1], the problem was solved with the use of laser-induced fluorescence of photo fragments at $\lambda = 247.85$ nm. The limit of detection (LOD) of 10^{-14} g/cm³ for trinitrotoluene vapors (TNT) was obtained by registering the luminescence of NO-fragments of fragmented TNT molecules during the detection time of 10 s from a distance of several meters. The developed system is bulky, and laser remote irradiation is not safe, so the method is not convenient for practical usage. Another approach to detecting vapors of explosives involved their concentration on meshes with subsequent thermal desorption and analysis in a portable chromatograph with polycapillary columns and air as carrier gas; an LOD of 10^{-14} g/cm³ was obtained in this case [2]. In [3], a standoff Raman spectrometer capable of detecting explosives at distances of 27 and 50 m was created. A YAG:Nd³⁺ laser with doubled frequency of radiation (532 nm) was used in the system. The authors estimated the LOD of the system as 250 ppm with an integration time of 100 s. The technology related to quenching of luminescence of amplifying fluorescent polymers allowed the LOD comparable to the LOD of trained dogs around 10^{-16} g/cm³ to be reached, and the technology was brought to practical use [4].

Ion mobility spectrometry instrumentation (IMS) as gas analytical technology is today one of the few practically applied in the sphere of detecting vapors of explosive substances. It is widely applied in the area of transport security and counterterrorism. The most commonly used vapor phase ionization methods are corona discharge and radioactive ^{63}Ni ; however, these methods do not demonstrate high selectivity. The limit of detection (LOD) of state-of-the-art IMS is around 10^{-14} g/cm³ (ppt level). The current goal for analytical instrumentation is to achieve the ability to detect explosives with extremely low volatility and a saturated vapor concentration level of 10^{-14} g/cm³. The presence of winds and air convection results in vapor dilution down to 10^{-15} g/cm³ and less, recognizable only by trained dogs. Thus, the LOD needs to be decreased down to 10^{-15} – 10^{-16} g/cm³. Further progress for distinguishing lower concentrations of explosive vapors is, however, limited by ionization mechanisms involved in particular ion formation processes. UV laser ionization source can be a very promising way to enhance sensitivity of ion mobility spectrometers due to its flexibility in terms of tunable wavelength, repetition rate, power and intensity. Today, atmospheric ion formation processes under laser radiation and parameters of laser radiation that can maximize ionization efficiency of explosives have not yet been completely studied.

The most detailed information in current knowledge about laser ionization is about the range of wavelengths suitable for effective ionization achievable by small size laser sources that can be positioned inside portable ion mobility spectrometers. The most commonly used lasers emit in the ultraviolet range, as UV radiation is effectively absorbed by molecules of nitro compounds, particularly trinitrotoluene (TNT), cyclotrimethylenetrinitramine (RDX), cyclotetramethylene-tetranitramine (HMX) and pentaerythritol tetranitrate (PETN) [5,6]. Excimer lasers are not suitable for portable devices because of their high production costs and large size and weight. Small size semiconductor laser diodes are incapable of generating high energy pulses for effective photoionization. A compact and relatively lightweight technical solution can be provided by solid state pulsed lasers with second and fourth harmonic generation. Such kinds of laser sources can emit radiation with peak power exceeding 10^6 W/cm² at a wavelength of $\lambda = 266$ nm. These properties make solid state lasers preferable as ionization sources in analytical instrumentation.

The process of formation of negative ions of organic nitro molecules under laser irradiation ($\lambda \geq 266$ nm) at atmospheric pressure and unpurified air remains understudied. Direct one- and two-quantum ionization of the main components of air and inorganic impurities (O₂, N₂, CO₂, CO, NO₂, N₂O) is impossible (ionization potentials exceed 11.3 eV) [7]. Presumably, the process starts through two-quantum resonance-enhanced multiphoton or multistage ionization (REMPI) of air impurities—basically organic molecules—(C_nH_m, benzene, ethylbenzene, trimethylbenzene and NO) present in the air [8], transfer of released electrons to molecules of nitro-compounds through ion-molecular reactions involving oxygen-water clusters. Such reactions usually cause formation of a negatively charged (M⁻) or negatively charged deprotonated molecule of nitro compound (M-H)⁻ [9,10]. Another difference to traditional mechanisms of ionization can be REMPI of nitro molecules themselves. This process can take place due to a sufficiently complex photophysics of electronic excitation between singlet and triplet states of nitro-molecules [11,12]. However, the contribution of this method of direct ionization of nitro-molecules to negative ion formation has not yet been studied.

Previously published results [13,14] revealed the optical parameters of laser ionization of TNT and RDX. Optimal laser radiation intensity for TNT was estimated and 3×10^7 W/cm² and for RDX 7×10^7 W/cm² wherein laser ion mobility spectrometry achieved an LOD of 10^{-14} – 10^{-15} g/cm³ for TNT [15]. However, the universality of application of the spectrometer is aimed to detect not only TNT, but also other explosives, whereas laser radiation parameters, optimal for one substance, can provide poor ionization for another one. There are no results for laser parameters optimal for detection of HMX and PETN. Furthermore, there are no estimates of limits of detection for RDX, HMX and PETN achievable at laser ionization. A comparison of laser ionization source and beta radiation for PETN and HMX is also not presented in published works.

The purpose of this work is to determine optimal parameters of laser radiation for negative ion formation of nitro group-based explosives using the examples of TNT, RDX, HMX and PETN at atmospheric pressure and ambient unpurified air; compare laser ionization source and ^{63}Ni beta radiation source in terms of efficiency and ionization mechanisms; and demonstrate the possibility to achieve lower limits of detection than for traditional ionization sources with the further prospect of creating highly sensitive portable explosives detectors.

2. Materials and Methods

2.1. Reagents

Chemically pure trinitrotoluene (TNT), cyclotrimethylenetrinitramine (RDX), cyclotetramethylenetetranitramine (HMX) and pentaerythritol tetranitrate (PETN), 99% were used in an experimental study. These analytes were synthesized in D. Mendeleev University of Chemical Technology of Russia and intended for analytical device certification and calibration purposes according to the procedure established in the Russian Federation. Solutions having concentrations of 10 mg/mL for each of the chemicals were prepared in chemically pure acetonitrile (by Chimmed, 99.9%). All the samples were prepared by depositing 1 mL (10 mg of solid substance) of each solution on the inner surface of stainless steel vapor generators. Each solution was dried at room temperature to form a homogeneous layer of solid analyte over a period of 7 days.

2.2. Apparatus

A field asymmetric ion mobility spectrometer (FAIMS) with cylindrical separation chamber (“shelf”) was used to obtain differential ion mobility spectra (Figure 1a, Table 1).

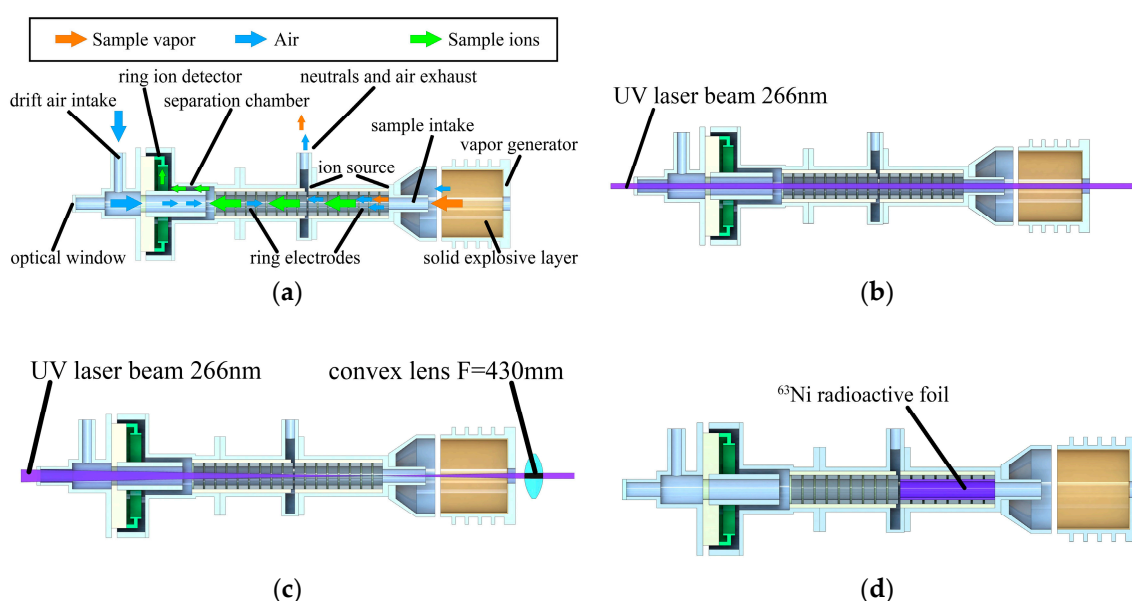


Figure 1. Schemes of field asymmetric ion mobility spectrometer (FAIMS): (a) Scheme of air, sample and ion flows inside FAIMS; (b) scheme of laser beam coaxial to ion source; (c) scheme of laser beam focusing and defocusing with convex lens; (d) scheme of placement of nickel radioactive foil inside ion source of the spectrometer.

Two types of ionization sources were used in the experiment: laser beam passing through the hole at the bottom of vapor generator (Figure 1b) and ^{63}Ni beta radioactive foil covering the ion source internal surface (Figure 1d). A Nd $^{3+}$:YAG laser source with 4-th harmonic $\lambda = 266$ nm, pulse duration $\tau = 6$ ns, variable pulse energy up to 2.5 mJ and pulse repetition rate of 10 Hz (Solar Systems LQ-215) and parallel laser beam diameter of 0.8 mm was used in experimental setup (Figure 1c). A movable

UV transparent convex lens with $F = 430$ mm was used for focusing and defocusing the laser beam inside the FAIMS ion source. The lens mount was 3D printed (Designer X Pro, Picaso 3D, Moscow, Russia) from UV absorbing plastic (Formax, REC, Moscow, Russia). A carriage with lens mount was attached to an aluminum rail with a tunable position to achieve perfect alignment with the ion path and ion source of the spectrometer in the whole range of distances.

Table 1. Technical parameters of FAIMS.

Parameter	Value
Sample intake diameter	7 mm
Ion source diameter	7 mm
Ion source length	45 mm
Separator length	65 mm
Outer electrode diameter	14 mm
Electrode gap width	2.5 mm
Separation voltage frequency	1 kHz
Separation voltage range	2000–3000 V
Compensation voltage range	−90 to +90 V
Detector current range	1×10^{-15} – 6×10^{-11} A
Linear dynamic range ¹	1×10^{-15} – 1×10^{-11} A
Resolution (FWHM) ²	2–15
Detector settling time	0.2 s
Input impedance	$4.7 \times 10^9 \Omega$
Maximum intake gas flow	500 cm ³ /min
Drift gas flow	1300 cm ³ /min

¹ Depends on ion type; ² depends on ion type and separation voltage.

Vapor generators were heated with a thermoelectric module (TB-41-1.0-0.8CH). A multimeter (APPA 502, APPA Tech. Corp., New Taipei City, Taiwan) with a metal thermocouple was used for monitoring the temperature of the vapor generator and the voltage signal from the relative humidity sensor (HIH-4000-001, Honeywell, Charlotte, NC, USA) inside the drift chamber. External ambient temperature and humidity were monitored with a combined temperature and humidity meter (DT-191A, CEMTech., Shenzhen, China). An Ophir NOVA II power meter was used to control average laser power and pulse energy.

2.3. Experimental Procedure

The experimental study included three parts:

1. Measurement of differential ion mobility spectra at varying separating fields
2. Measurement of the ion current at the center of the ion peak of each substance at varying laser beam intensities
3. Estimation of LOD for each of the substances

2.3.1. Measurements of Differential Ion Mobility Spectra

Measurements of differential mobility spectra were done at atmospheric pressure of 740–760 Torr under controlled ambient temperature of 25 °C and ambient relative humidity of 30%; these atmospheric conditions were stabilized with a climate control system inside the laboratory. FAIMS was set to 300 cm³/min sample intake flow. Relative humidity inside the drift air intake (1300 cm³/min) was controlled to be equal to the ambient humidity (30%). This control was achieved by separating the flow of drift air into two parts. The first part was dried with silica gel granules. The second part was humidified by blowing air above the water surface. The two parts were further mixed in tunable proportions forming air with controlled relative humidity measured with a humidity sensor. Each stainless steel vapor generator with an attached heater was placed in front of the FAIMS sample

intake coaxially at a distance of 2 mm to provide steady airflow with a constant concentration of analyte, giving ion current repeatability within a 200 fA range. The TNT generator was kept at 25 °C without heating. The RDX and HMX generators were heated to 50 °C, PETN was heated to 45 °C, and the temperature was controlled by a thermocouple connected to a multimeter during the whole experiment. All the temperatures were well below the thermal decomposition limit and were chosen in order to create a vapor concentration high enough for distinct signal acquisition. Concentrations were calculated from Raoult's law equations in [16]: $C_{25 \text{ TNT}} = 6.6 \times 10^{-11} \text{ g/cm}^3$; $C_{50 \text{ RDX}} = 2 \times 10^{-12} \text{ g/cm}^3$; $C_{45 \text{ PETN}} = 6 \times 10^{-12} \text{ g/cm}^3$; $C_{50 \text{ HMX}} \approx 10^{-17} \text{ g/cm}^3$ (probably direct calculation is not applicable in the case of HMX). Temperature stability was within a 3 °C range. When β -radiation was used, ^{63}Ni foil was installed inside the ion source (Figure 1d) to irradiate the whole volume inside it; the laser was turned off. When laser ionization was used, the ^{63}Ni foil was removed, and a parallel laser beam with a diameter of 0.8 mm (Figure 1b) was aligned coaxially with the cylindrical surface of the ion source and with a vapor generator. The laser was set to 10 Hz repetition rate, the pulse energy was set to 1.5 mJ, and the resulting intensity was $5 \times 10^7 \text{ W/cm}^2$. Molecules in the vapor sample from the generator were ionized inside the ion source, and ion spectra were recorded from 0 V (0 Td) to 25 V (0.37 Td) compensation voltage for separating voltages within the 2000–3000 V range (30–45 Td), changed with steps of 50 V (0.75 Td). Spectra for each value of separating voltage were recorded 5 times for averaging. These measurements were conducted the same way for both laser ionization and for ^{63}Ni ionization. Well-controlled ambient conditions and uniform humidity outside and inside the spectrometer gave intra-day repeatability within the 200 fA range for all the peaks. Laser pulse energy measurement during the working day demonstrated that the chosen ambient temperature provided the most stable laser performance, with energy fluctuation within a 5% range. Recording of the spectra at reproduced humidity and temperature with several days interval did not show any noticeable peak shift along the compensation voltage axis, which was confirmed by aligning the reactant peaks from different series of measurements carried out within several weeks.

2.3.2. Measurement of Ion Current at Varying Laser Beam Intensities

Atmospheric conditions in this part of the experiment were kept the same as in previous part. In order to maximize temperature stability inside the laser, the laboratory climate control system was set to minimum air flow. This allowed the laser power and therefore pulse energy to be kept within a 5% range during all the measurement series. The laser pulse energy was changed with an attenuator in the entire range and was checked after each of the measurement series. Each of the vapor generators was installed the same way as in the previous part. Laser radiation intensity at constant pulse energy was controlled by focusing and defocusing the beam with a convex lens with a focal distance of 430 mm, providing a beam with a nearly constant diameter along the whole ion source (Figure 1c). The spectrometer was set to 300 cm³/min sample intake flow, 3000 V (45 Td) separation voltage and a compensation voltage range of 1.5 V around the center of the ion peak of the measured substance. The spectra at each value of energy and irradiated volume inside the ion source were recorded repeatedly to minimize ion current fluctuations by averaging the results. Background spectra without vapors of analytes were recorded and subtracted from spectra with presence of analytes to acquire only the contribution of ions of nitro-compounds. In order to prevent any influence of vapors absorbed inside the spectrometer, background spectra were recorded only after blowing the internal ion path with air and heating it to $t = 80 \text{ °C}$ for 1 h.

2.3.3. Estimation of LOD for Each of the Substances

The limits of detection for RDX, PETN and HMX were measured at room temperature of 25 °C. FAIMS was set to maximum intake air flow of 500 cm³/min and a 30 Td separation field, and the laser beam was introduced from the opposite side of the device through an optical window (from left to right at Figure 1b). The open side of the detector was covered by a laser radiation absorber with holes for air and sample introduction.

Saturated vapor of explosives was prepared by depositing dry explosives on a solid base placed into 1000 cm³ plastic bags, kept closed for 5 days at 25 °C in order to achieve equilibrium concentration. When capturing the amplitude of the ion current from the saturated vapor of explosives, the plastic bags were attached tightly to the sampling intake of the detector for 1 min, which was enough for recording the spectra without changes in vapor concentration. When pumping air out of the bag by the FAIMS, its volume was reduced to half of its initial volume. The recording of spectra began with the 10th second after the package was attached to the sampling intake. In each measurement, 5 spectra were recorded to control concentration stability. The concentration value of saturated vapors was determined by Raoult's law equations from [16]. After each measurement, the internal path of the spectrometer was heated at $t = 80$ °C and blown for 1 h. The purity control was carried out using the spectrum in the absence of the analyte.

3. Results

3.1. Ion Spectra for ⁶³Ni and Laser Sources and Separation Field Dependences

Ionization mechanisms of nitro-compounds depend on ionization conditions (type of ion source and gas composition). Generally, in air for ⁶³Ni, the reactant ions in negative polarity are O₂⁻, O₂⁻(H₂O), O₂⁻(H₂O)₂, CO₂⁻, CO₄⁻ and their hydrates [17]. According to [18,19], ⁶³Ni, corona discharge and electrospray ionization form TNT-H⁻ ion for TNT, PETN+NO₃⁻ for PETN, RDX+NO₂⁻ and 2RDX+NO₂⁻ for RDX, HMX+NO₂⁻ and HMX+NO₃⁻ for HMX. The peak of TNT (Figure 2a) demonstrated that ions formed at laser ionization were at the same compensation field as ions formed at ⁶³Ni ionization, but the composition of reactant ions was to some extent different (Figure 2a). The same situation was observed for PETN (Figure 2c).

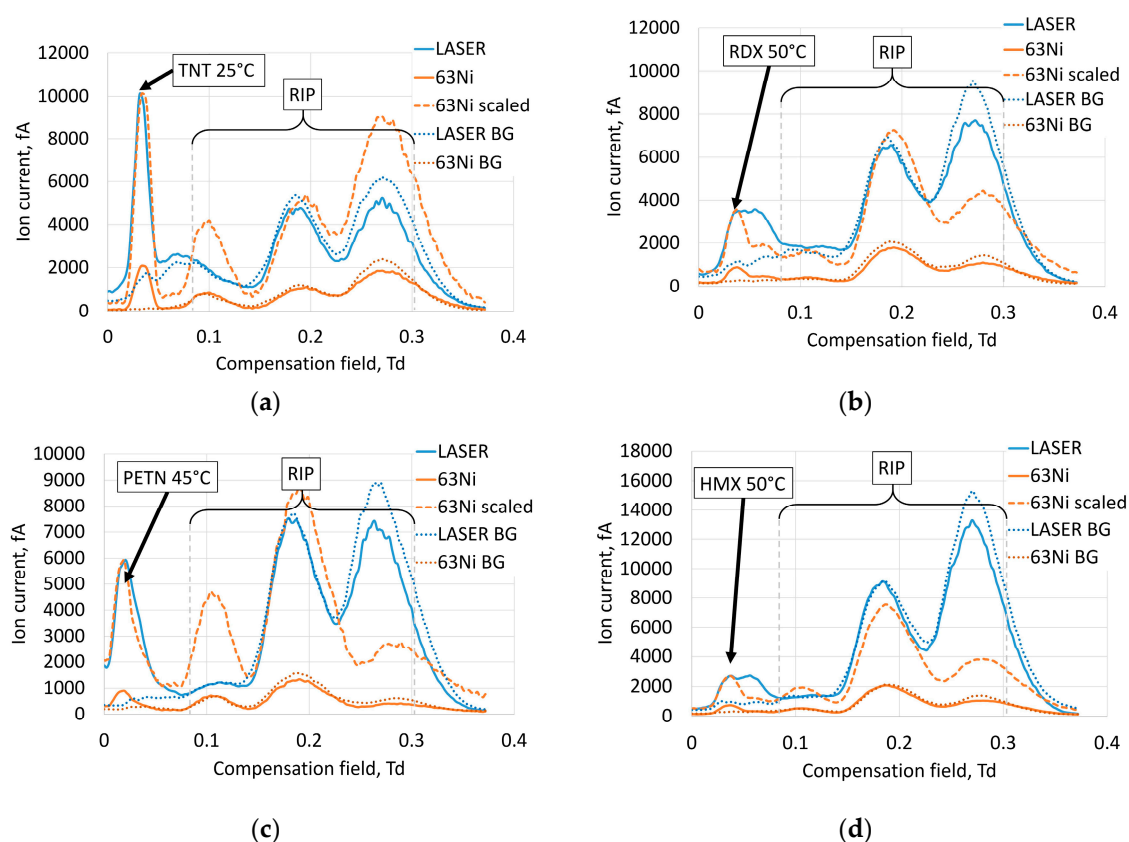


Figure 2. Comparison of ion mobility spectra at separation field of 45 Td from laser at $I = 3.5 \times 10^7$ W/cm² and ⁶³Ni ionization: (a) TNT at 25 °C; (b) RDX at 50 °C; (c) PETN at 45 °C; (d) HMX at 50 °C.

This also corresponded to the dependence of the compensation field at the center of the peaks of TNT and PETN from the separation field (Figure 3a,c). Thus, it is highly probable that the laser ion source forms the dominating TNT-H⁻ ion for TNT and PETN+NO₃⁻ for PETN. There was still a reactant peak at 0.1 Td at ⁶³Ni ionization that was not present at laser ionization, which means that the laser produced less reactant ions and was a more selective ion source.

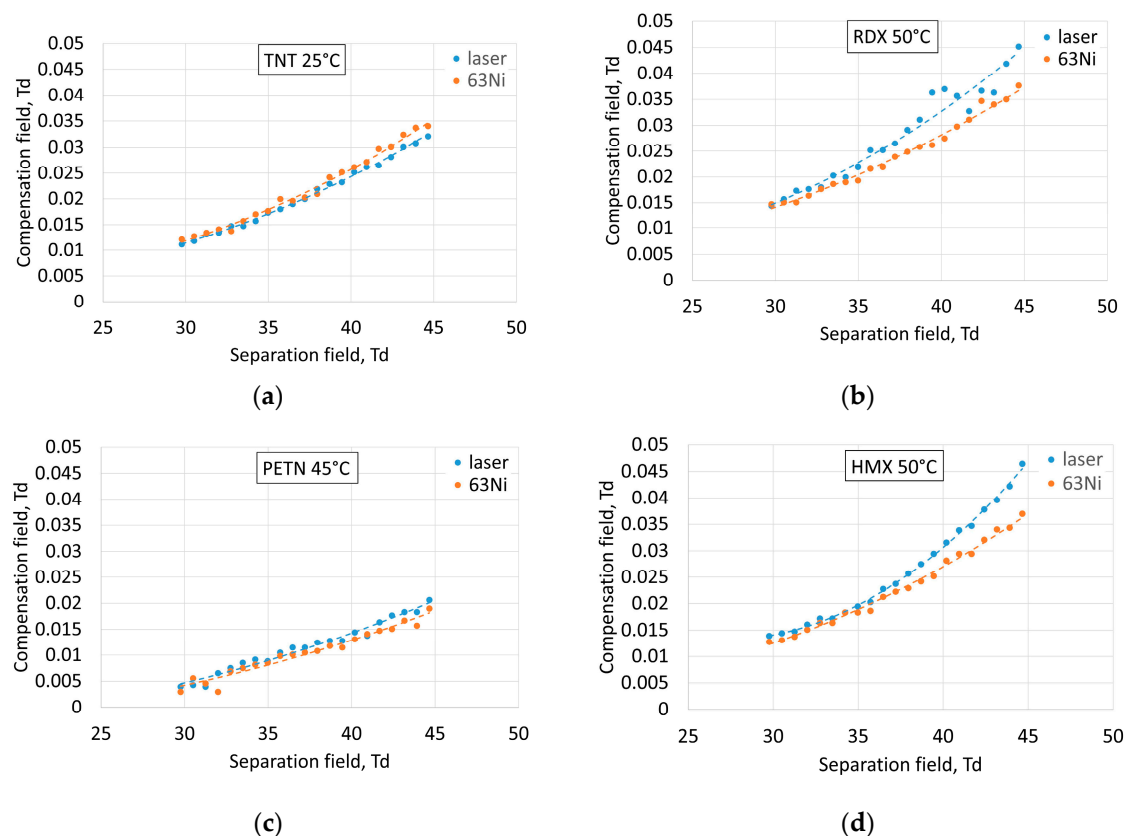


Figure 3. Comparison of ion peak positions at separation field variation from laser at $I = 3.5 \times 10^7 \text{ W/cm}^2$ and ⁶³Ni ionization: (a) TNT at 25 °C; (b) RDX at 50 °C; (c) PETN at 45 °C; (d) HMX at 50 °C. Рис.3.

Comparison of spectra (Figure 2b,c) demonstrates that RDX and HMX peaks significantly differed for ⁶³Ni and the laser. The dependence of compensation field values at the centers of the peaks of RDX and HMX on the separation field (Figure 3b,d) at laser ionization corresponded to a higher compensation field than at ⁶³Ni ionization. We can suppose that at both ionization sources, RDX+NO₂⁻ and HMX+NO₃⁻ dominated in the ion spectra of RDX and HMX, respectively. The laser ionization source showed that there was another type of ion for RDX and HMX that formed in similar amounts as RDX+NO₂⁻ and HMX+NO₃⁻, respectively. This demonstrated the difference in ionization mechanisms of nitramine ring compounds at laser and beta radiation. It is also important to note that implementation of two types of ion sources inside the same spectrometer at the same experimental conditions provided an opportunity to compare signal levels in both cases. Laser ionization provided a several times higher signal level than radioactive foil, which is considered to be a highly selective ionization source and is installed inside state-of-the-art commercially available detectors. Deeper understanding of ion formation processes could be achieved in further experiments with the introduction of ions formed at atmospheric pressure in a mass-spectrometer.

3.2. Ion Current as Function of Laser Pulse Energy

Dependences of ion currents from laser pulse energy at different volumes of illuminated space inside the ion source of the spectrometer (Figure 4) showed that focusing the laser beam (Figure 1c) and

increasing the intensity moved the saturation limit to lower laser pulse energies and lower saturated ion current.

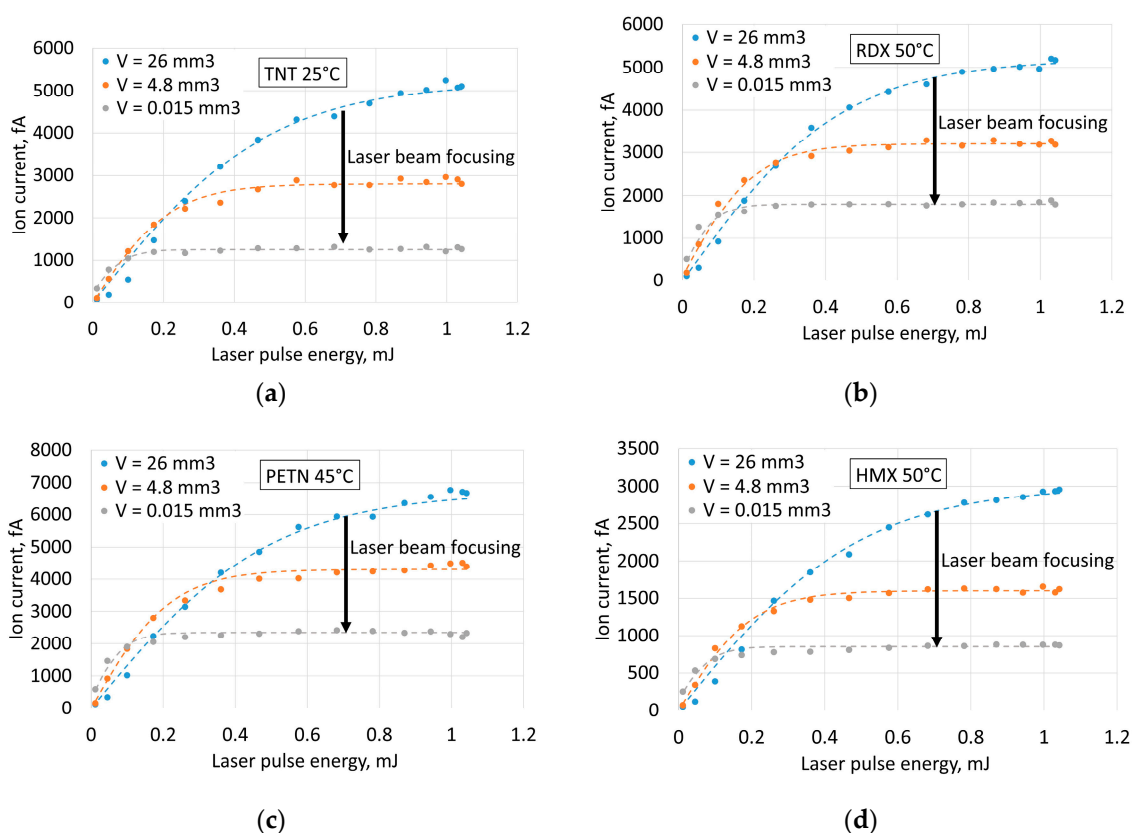


Figure 4. Amplitude of ion current in peaks of the explosives as a function of laser pulse energy at different volumes of illuminated space inside the ion source (beam volume): (a) TNT at 25 °C; (b) RDX at 50 °C; (c) PETN at 45 °C; (d) HMX at 50 °C.

The probable explanation of this effect is that the majority of the molecules in the sample become ionized and the ion current grows much slower with increased pulse energy.

3.3. Ion Current as Function of Volume of Illuminated Space

The fact of saturation of ion current at increasing laser pulse energy and influence of laser beam focusing on the saturation limit raises the question about the role of radiation intensity in the efficiency of ionization (Figure 5). The studies of mechanisms of ionization of nitro compounds regard them as indirect complex processes with ionization of organic impurities in the air at the first stage [20]. Variation of radiation intensity can influence this stage of the process. On the other hand, direct ionization is possible at high intensities as the probability of multiphoton processes becomes much higher. The decrease of the volume of irradiated space to increase laser intensity at given pulse energy, however, results in reduction of the number of ionized molecules. Therefore, for optimal parameters, it is necessary to maintain a fine balance between laser intensity (ionization probability), volume of illuminated space (number of molecules) and energy in the laser pulse (in practice, dimensions and power consumption of the laser). The optimal radiation intensity values for detecting all the explosives used are summarized in Table 2.

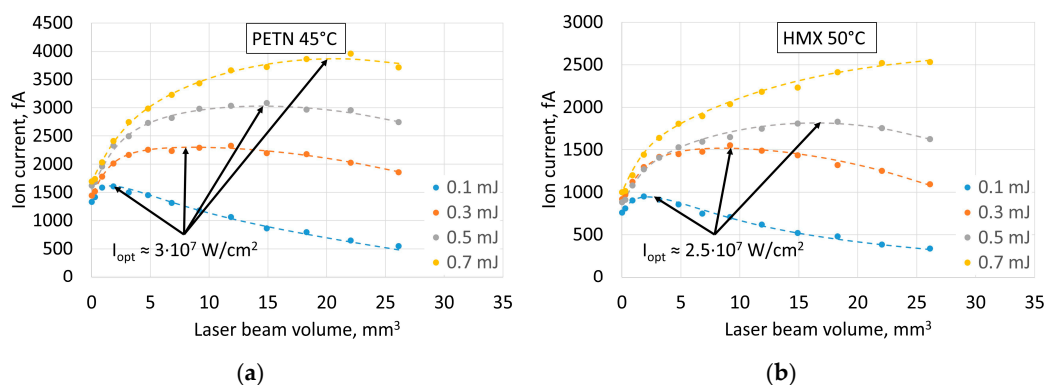


Figure 5. Amplitude of ion current in peaks of the explosives as function of volume of illuminated space inside ion source (beam volume) at different laser pulse energy: (a) PETN at 45 °C; (b) HMX at 50 °C.

Table 2. Optimal intensities for ionization of explosives in vapor phase.

Substance	$I_{opt}, W/cm^2$
TNT	3×10^7 [13]
RDX	7×10^7 [14]
PETN	3×10^7
HMX	2.5×10^7

3.4. Ion Current Amplitudes and Limits of Detection

According to previously published results [15] the estimated LOD of TNT vapor for laser FAIMS was $3 \times 10^{-15} \text{ g/cm}^3$. Current measurements of amplitude of the ion current from saturated vapor of explosives at room temperature of 25 °C gave us estimates of achievable signal to noise ratios for RDX, PETN and HMX (Figure 6). The optimal intensity of $4 \times 10^7 \text{ W/cm}^2$ was chosen as the average from TNT, RDX, PETN and HMX optimal intensities. Noise level was predominantly determined by properties of amplification circuit and atmospheric vapor non-uniformities, and mean square deviation was considered to be $\sigma \approx 200 \text{ fA}$. Table 3 shows signal to noise ratios. The minimum signal level at the LOD was considered to be $SNR_{LOD} = 2$. Considering the number of ions, captured by the detector proportional to vapor concentration, we can give a coarse estimate of the LOD from vapor concentration at experimental conditions. The limits of detection are shown in Table 3. Sorption of vapors inside saturated vapor generators can make vapor concentration lower than at saturation, but this means that we take the worst value, and the real LOD in this case was even lower. As for HMX, the published values of saturated vapor pressure are very controversial; however they are much lower than for RDX. This makes the reliable estimate of LOD difficult. The captured signal shows that the LOD for HMX is about five times lower than the saturated vapor concentration at 25 °C.

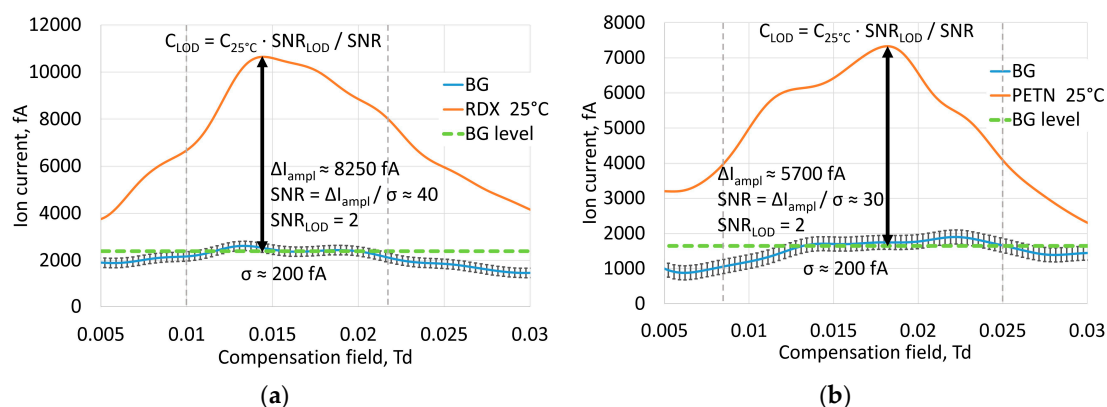


Figure 6. Cont.

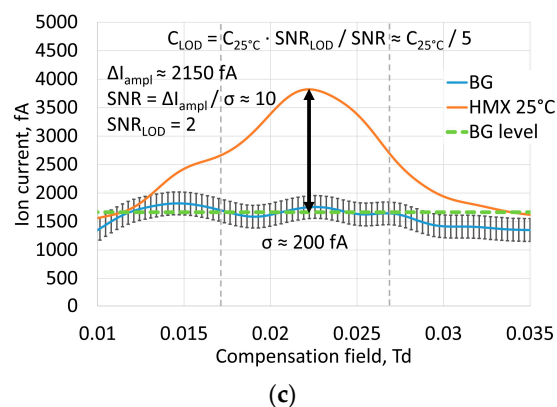


Figure 6. Amplitude of ion current in peaks from saturated vapor of the explosives at 25 °C: (a) RDX; (b) PETN; (c) HMX.

Table 3. Comparison of laser FAIMS capabilities of detecting explosives in vapor phase at 25 °C.

Substance	Ion Current Amplitude, fA	Signal to Noise Ratio (SNR)	Saturated Vapor Pressure, Torr	Calculated Vapor Density, g/cm ³	Estimated LOD, g/cm ³	Sample Utilization Ratio, C/mol
RDX	8250	40	3.3×10^{-9} [16]	6×10^{-14} [16]	2×10^{-15}	6×10^3
PETN	5700	30	1.16×10^{-8} [16]	1.2×10^{-13} [16]	9.3×10^{-15}	1.6×10^3
HMX	2150	10	3×10^{-15} [16]	3.6×10^{-20} [16]	$< 2 \times 10^{-15}$	$> 6 \times 10^3$

4. Discussion

The influence of laser pulse repetition rate on ionization processes was beyond the scope of this paper as this is mostly determined by the construction of the particular spectrometer and depends on the time necessary to fill the ionized volume with neutral molecules and update the sample. The detector used for this work has a sample update time about 20 ms [13], so the signal level is proportional to the laser repetition rate up to 50 Hz. Further increases in repetition rate results in ion current saturation. The repetition rate choice depends predominantly on the commercial availability and cost of lasers. Lasers with high peak frequencies are very expensive and heavy, while lasers with low operation repetition rate can have a much lower price and weight. The best solution will be a balance of laser intensity of about 4×10^7 W/cm², with a beam size covering enough space inside the ion source and a maximum repetition rate at a reasonable price, size and weight of the laser source. Optimization can make possible reduction of the weight of the developed laser FAIMS down to 4 kg with improved portability and operation time.

5. Conclusions

Since its inception about 40 years ago, ion mobility spectrometry has become a widely recognized, inexpensive and powerful analytical method for the detection of hazardous and prohibited substances under conditions of atmospheric pressure and temperature, monitoring of the air environment and production processes, medical diagnostics, pharmacology and forensic science.

One of the modern directions of the method development is improvement of analytical characteristics of ion mobility spectrometers in specific applications that require low LOD, high selectivity, sensitivity and identification ability.

In particular, the use of ion mobility spectrometers (IMS) for the detection of vapors of explosives is now clearly limited by their lack of sensitivity in relation to some practical explosives. The LOD of modern IMS and FAIMS with corona discharge ionization and β -radioisotope sources is no better than 10^{-14} g/cm³, which is clearly insufficient for direct detection of vapors of explosives, taking into account diffuse and convective phenomena. Therefore, in the case of real application, usually not vapors but traces of explosives in the pre-concentration mode are detected after wiping the object with tissues with subsequent heating and thermal desorption of adsorbate in the heating module. Reduced speed,

increased probability of false negative alarms and limited functionality of the detectors under this approach are obvious.

On the other hand, rapidity, mobility and the possibility of applying the ion method under atmospheric conditions are limited by the capabilities of the spectrometers. Due to the nature of atmospheric pressure chemical ionization (APCI), identification of components of multi-component gas mixtures is further complicated by the non-selectivity of the ionization sources used. In the case of detection of explosives, this results in a higher probability of false positive alarms, and the need for the combination of the IMS method with laboratory analysis methods.

This all means that analytical capabilities of ion mobility spectrometry method can be significantly improved by using solutions involving ionization sources that implement new or additional ionization mechanisms and have high selectivity, high sample utilization ratio and complementing IMS and FAIMS with new functionality.

In this work we achieved progress towards the improvement of performance of FAIMS by using a laser ionization source, where the radiation parameters were optimized for maximum ionization efficiency for the nitro group-based explosives TNT, RDX, HMX and PETN. We found that laser ionization source ($\lambda = 266$ nm) provides higher selectivity and a higher signal to noise ratio than radioactive ^{63}Ni at optimal intensity of laser radiation for PETN and HMX 3×10^7 W/cm² and 2.5×10^7 W/cm², respectively. It is necessary to maintain a fine balance between laser intensity (ionization probability), volume of irradiated space (number of molecules) and energy in the laser pulse (in practice, dimensions and power consumption of the laser) when constructing FAIMS with a laser ion source.

On the basis of the parameters found, we estimated LODs for the explosives used: 2×10^{-15} g/cm³ for RDX, 9×10^{-15} g/cm³ for PETN and less than 2×10^{-15} g/cm³ for HMX, which significantly exceeds the current range of IMS and FAIMS with non-laser ion sources.

Evaluation of other analytical parameters of the spectrometer and their further improvement is the subject of future work, as well as creation of a reliable explosive vapor detector with laser ionization.

Author Contributions: Conceptualization, A.A.C. and G.E.K.; validation, A.E.A.; investigation, V.A.K.; writing—original draft preparation and visualization, V.A.K.; supervision, resources and project administration, G.E.K. All authors have read and agreed to the published version of the manuscript.

Funding: This research was funded by RFBR (Russian Foundation for Basic Research), grant number 19-32-90280.

Conflicts of Interest: The authors declare no conflict of interest.

References

1. Bobrovnikov, S.; Vorozhtsov, A.B.; Gorlov, E.; Zharkov, V.; Maksimov, E.M.; Panchenko, Y.N.; Sakovich, G.V. Lidar Detection of Explosive Vapors in the Atmosphere. *Russ. Phys. J.* **2016**, *58*, 1217–1225. [[CrossRef](#)]
2. Baldin, M.N.; Gruzov, V.M. A portable gas chromatograph with air carrier gas for the determination of explosive traces. *J. Anal. Chem.* **2013**, *68*, 1002–1006. [[CrossRef](#)]
3. Carter, J.C.; Angel, S.M.; Lawrence-Snyder, M.; Scaffidi, J.; Whipple, R.E.; Reynolds, J.G. Standoff Detection of High Explosive Materials at 50 Meters in Ambient Light Conditions Using a Small Raman Instrument. *Appl. Spectrosc.* **2005**, *59*, 769–775. [[CrossRef](#)] [[PubMed](#)]
4. Rochat, S.; Swager, T.M. Conjugated Amplifying Polymers for Optical Sensing Applications. *ACS Appl. Mater. Interfaces* **2013**, *5*, 4488–4502. [[CrossRef](#)] [[PubMed](#)]
5. Schroeder, W.A.; Wilcox, P.E.; Trueblood, K.N.; Dekker, A.O. Ultraviolet and Visible Absorption Spectra in Ethyl Alcohol. *Anal. Chem.* **1951**, *23*, 1740–1747. [[CrossRef](#)]
6. Feagin, T.A.; Rae, P.J. Optical absorption in polycrystalline PETN, RDX, HMX, CL-20 and HNS and its possible effect on exploding bridgewire detonator function. *J. Energetic Mater.* **2020**, 1–11. [[CrossRef](#)]
7. Buryakov, I.A. Detection of explosives by ion mobility spectrometry. *J. Anal. Chem.* **2011**, *66*, 674–694. [[CrossRef](#)]
8. Vilesov, F.I. Photoionization of gases and vapors by vacuum ultraviolet radiation. *Sov. Phys. Usp.* **1964**, *6*, 888–929. [[CrossRef](#)]

9. Kotkovskii, G.E.; Tugaenko, A.V.; Chistyakov, A.A. Negative ion formation in laser ion mobility increment spectrometer. *Tech. Phys. Lett.* **2010**, *36*, 276–278. [[CrossRef](#)]
10. Martynov, I.; Karavanskii, V.A.; Kotkovskii, G.E.; Kuzishchin, Y.A.; Tsybin, A.S.; Chistyakov, A.A. Ion mobility spectrometer with ion source based on laser-irradiated porous silicon. *Tech. Phys. Lett.* **2011**, *37*, 15–18. [[CrossRef](#)]
11. Artyukhovich, A.N.; Bykovsky, Y.A.; Chistyakov, A.A.; Potapov, M.M. Superrapid Intersystem Crossing in Time-Selective Laser Action on Nitroaromatic Crystals. *Laser Phys.* **1992**, *2*, 372–382.
12. Artyukhovich, A.N.; Bykovsky, Y.A.; Chistyakov, A.A.; Potapov, M.M. Intersystem Crossing in Processes of Power Resonant Laser Action in Nitroaromatic Crystals. *Zh. Prikl. Spektrosk.* **1998**, *50*, 595–600.
13. Akmalov, A.E.; Chistyakov, A.A.; Kotkovskii, G.E.; Kostarev, V.A. Parameters of laser ionization of explosives for ion mobility spectrometry. *Proc. SPIE* **2018**, 10802. [[CrossRef](#)]
14. Akmalov, A.; Chistyakov, A.A.; Kotkovskii, G.E.; Kostarev, V.A. Detection of vapors of explosives by field asymmetric ion mobility spectrometry method with laser ionization. *Proc. SPIE* **2019**, 11166, 2.
15. Chistyakov, A.A.; Kotkovskii, G.E.; Sychev, A.V.; Odulo, I.P.; Bogdanov, A.S.; Perederiy, A.N.; Shestakov, A.V. A Picosecond Laser FAIMS Analyzer for Detecting Ultralow Quantities of Explosives. *Proc. SPIE* **2014**, 9253, 2.
16. Östmark, H.; Wallin, S.; Ang, H.G. Vapor Pressure of Explosives: A Critical Review. *Propellants Explos. Pyrotech.* **2012**, *37*, 12–23. [[CrossRef](#)]
17. Eiceman, G.; Schmidt, H.; Cagan, A.A. Explosives detection using differential mobility spectrometry. In *Counterterrorist Techniques Detection of Explosives*; Yinon, J., Ed.; Elsevier: Amsterdam, The Netherlands, 2007; pp. 63–88.
18. Cheng, S.; Dou, J.; Wang, W.; Chen, C.; Hua, L.; Zhou, Q.; Hou, K.; Li, J.; Li, H. Dopant-Assisted Negative Photoionization Ion Mobility Spectrometry for Sensitive Detection of Explosives. *Anal. Chem.* **2012**, *85*, 319–326. [[CrossRef](#)] [[PubMed](#)]
19. Du, Z.; Sun, T.; Zhao, J.; Wang, D.; Zhang, Z.; Yu, W. Development of a plug-type IMS-MS instrument and its applications in resolving problems existing in in-situ detection of illicit drugs and explosives by IMS. *Talanta* **2018**, *184*, 65–72. [[CrossRef](#)] [[PubMed](#)]
20. Martynov, I.L. Mechanisms of Formation of Ions of Nitroaromatic Molecules in the Gas Phase and on the Surface of Porous Silicon under UV-Laser Influence. Ph.D. Thesis, Moscow Engineering Physics Institute, Moscow, Russia, 2011.



© 2020 by the authors. Licensee MDPI, Basel, Switzerland. This article is an open access article distributed under the terms and conditions of the Creative Commons Attribution (CC BY) license (<http://creativecommons.org/licenses/by/4.0/>).